Received: 4 March 2023 | Revised: 5 May 2023 | Accepted: 19 May 2023

DOI: 10.1111/ijac.14463

International Journal of Applied Ceramic Technology

RESEARCH ARTICLE

Enhancing magnetic levitation and guidance force and weight efficiency of high-temperature superconducting maglev systems by using sliced bulk YBCO

Murat Abdioglu[1,2] | **U. Kemal Ozturk**[1] | **Sait Baris Guner**[1,3] | **Mehmet Ozturk**[4] | **Hakki Mollahasanoglu**[1,5] | **Ekrem Yanmaz**[6]

[1]Department of Physics, Faculty of Science, Electromagnetic Guidance and Acceleration Research Group (EMGA), Karadeniz Technical University, Trabzon, Türkiye

[2]Department of Mathematics and Science Education, Faculty of Education, Bayburt University, Bayburt, Türkiye

[3]Department of Physics, Faculty of Art and Science, Recep Tayyip Erdoğan University, Rize, Türkiye

[4]Department of Electrical and Electronics Engineering, Faculty of Engineering, Karadeniz Technical University, Trabzon, Türkiye

[5]Department of Electrical-Electronics Engineering, Faculty of Engineering and Architecture, Recep Tayyip Erdoğan University, Rize, Türkiye

[6]Department of Electrical and Electronics Engineering, Faculty of Engineering and Architecture, Nisantasi University, Istanbul, Türkiye

Correspondence
Murat Abdioglu, Department of Physics, Faculty of Science, Electromagnetic Guidance and Acceleration Research Group (EMGA), Karadeniz Technical University, 61080, Trabzon, Türkiye.
Email: muratabdioglu61@gmail.com

Funding information
Scientific and Technological Research Council of Türkiye (TUBITAK), Grant/Award Number: 122F432; Scientific Research Projects Coordination Unit of Karadeniz Technical University, Grant/Award Number: FBA-2021-9814

Abstract

We aimed to enhance the magnetic force efficiency of Maglev systems without increasing total weight. For this aim, we divided YBCO bulks into three slices horizontally to utilize the YBCO-permanent magnetic guideway (PMG) interaction surface as much as possible. We used whole YBCO above PMGs with different magnetic pole directions (PMG-A and PMG-B) in two lying positions of transversal and longitudinal and investigated levitation and guidance force performances. It is determined that levitation and guidance forces by using YBCO in transversal lying mode are bigger compared to the longitudinal mode. For sliced YBCO, the maximum levitation force increased by 69% and 78%, while the guidance force enhancements are determined as 212% and 91%, compared to the whole YBCO above PMG-A and PMG-B, respectively. The levitation and guidance force density with respect to the total mass of unit a set of slices YBCO increased by 92% and 106%, respectively, compared to the whole YBCO above PMG-B in transversal mode. Since the higher levitation force and the lower total weight of the onboard unit are important parameters in point of the energy efficiency in Maglev and other levitation applications, the result of this study supplies useful data for the engineers and industrial partners.

KEYWORDS
levitation force, maglev, porosity analysis, sliced YBCO

1 | INTRODUCTION

The researchers' attention on the REBCO (RE = Rare Earth) high-temperature superconducting (HTS) materials[1] has been increasing due to their strong diamagnetism behaviour in addition to their high flux pinning ability in an external magnetic field. These properties provide a unique self-stabilization to these materials enabling them to play a vital role in levitation systems such as magnetic levitation vehicles (Maglev),[2–5] flywheel energy storage systems,[6,7] magnetic bearings,[8] motors,[9,10] generators,[9] magnet applications,[11–13] and so forth. The mentioned systems use REBCO materials in wire, tape or bulk forms as needed. In the current studies on Maglev systems as one of the outstanding applications, mainly YBCO materials have been exploited as HTS in bulk form due to their passive stable levitation behaviour.[14–17] The levitation force performance of Maglev systems robustly depends on the external magnetic field source and superconducting properties of the HTS materials according to the general formula given as $F = m\,\partial H/\partial z$, where $\partial H/\partial z$ is the external magnetic field gradient and m is magnetic moment depending on the supercurrent density.[18] Therefore, researchers have concentrated on optimising the permanent magnetic guideway (PMG) used as an external magnetic field source and fabricating HTS materials in excellent quality as much as possible. Excellent quality means having high flux trapping ability and high critical current density. In addition to these features, YBCO materials are desired as large as possible in real-scale applications. However, producing HTS materials in large dimensions is an extremely challenging procedure and takes too long due to the low rate of crystal growth.[19]

The first solution to overcome this challenge is the top-seeded-melt-growth (TSMG) method, in which a seed is used on the material to be grown with a higher melting temperature than this material.[20,21] During the ongoing studies, the multi-seeded-melt-growth (MSMG) technic has been developed in which more than one seed is used on the material to produce larger-sized single-grain HTSs in different dimensions and geometries.[18,19,22] Different studies have been performed to enhance the superconducting material properties in addition to the size of the bulk REBCO, such as using a cylindrical[23,24] or pyramid-like[25] buffer layer between the seed and the main material. Notwithstanding the numerous number of studies done so far, the most commonly used bulk YBCO in Maglev studies of laboratory scale[14,15,26] or real-scale prototypes[5,27] are the ones fabricated by ATZ GmbH[8,22,28–30] in a rectangular prism shape with three seeds.

In addition to the efforts to enhance the structural properties of bulk YBCO, there are studies in the literature to enhance the macro superconducting properties such as levitation force by using three seeded YBCOs mentioned above, in different configurations or orientations. Deng et al. conducted a study to improve the levitation and guidance performance of Maglev systems by changing the laying mode of the HTS above the PMG.[26] Researchers used four numbers of the same YBCO bulks in different arrays above two different PMGs to investigate the levitation force performance of the Maglev system[31] As well as the studies based on the HTS, researchers also focused on the PMG side in magnetic rail. But there are commonly used two types of PMGs, conventional[32] and Halbach types,[33] and there is little left to do anymore to optimise them except for increasing the number of permanent magnets (PM). An effective method to increase the levitation efficiency is hybrid systems in which the PMs are used on the onboard side together with the HTSs.[34–36] This method utilises the bigger repulsive force interaction between the PMG and auxiliary onboard PMs. On the other hand, the PMG installation cost is a large part of the installation budget of the system as it is laid along kilometres of rails. Therefore, multi-surface HTS-PMG interactions have been offered in previous studies as a good way to enhance the levitation and guidance performance without increasing the PMG construction cost.[36,37]

In all levitation systems, the weight of the system is an important parameter since it affects the energy efficiency of the Maglev vehicles or the delivered power density of the motors and generators. Therefore, the total HTS number in the system and total weight have to be decreased without decreasing the force performance. In this study, as different from the studies conducted so far, we have aimed to utilize the PMG surface as much as possible to enhance the force performance of Maglev systems without increasing HTS or PM number. For this aim, we have divided YBCO bulks into three slices horizontally, thus tripling the HTS surface interacting with the PMG, and investigated the magnetic levitation and guidance performance and magnetic stiffness of HTS Maglev systems. Firstly, we have obtained the magnetic flux density distribution of the used three different PMG arrangements numerically via magnetostatic solution in COMSOL Multiphysics. Then, we experimentally determined the most effective PMG arrangements, in point of magnetic force and force density performance, for one whole bulk YBCO as a reference sample and the sliced YBCO pieces. Finally, we compared the levitation and guidance force results of one whole YBCO and three sliced pieces of one YBCO. It is concluded that the levitation force performance can be increased in addition to the huge increment in the guidance force by slicing one

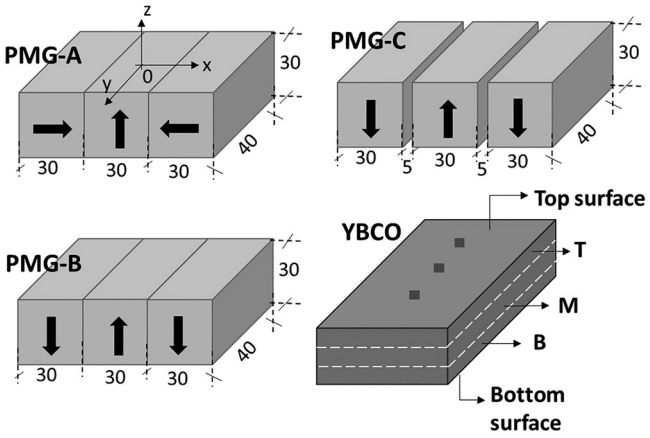

FIGURE 1 Schematic view of three different permanent magnetic guideway (PMG) arrangements and bulk YBCO (three-seeded sample) with the horizontal slice lines.

YBCO into three pieces and thus increasing the interaction surface of the YBCO with the PMG.

2 | EXPERIMENTAL PROCEDURE

The image analysis procedure consists of acquiring images and digital image processing parts, namely segmentation. The acquisition of the photos is conducted with a high-resolution RGB camera. After loading these photos into the computer, the acquired RGB images are converted to grayscale images for the segmentation part in MATLAB software. The segmentation process is done with a local thresholding algorithm. This algorithm adaptively segments the background (holes) and foreground into two classes based on intensity levels. After segmentation, some morphological image processing steps are applied to the segmented objects to eliminate false segmentation results. The morphological operations calculate the objects' "EquivDiameter", "Solidity" and "Eccentricity" properties.

The schematic view of three different PMG arrangements and bulk YBCO (three-seeded samples) used in this study is shown in Figure 1. NdFeB PMs of N42 grade are in dimensions and have surface magnetic flux densities of 40 mm × 30 mm × 30 mm and 0.53 T, respectively. The three-seeded YBCOs are fabricated by ATZ GmbH with final dimensions and mass after the heat treatment of 65 × 33 × 13 mm and 172 g, respectively. Three HTSs were sliced horizontally into three pieces, top (T), middle (M), and bottom (T), by using a circular diamond saw in a precision cutting machine. The levitation force, guidance, and magnetic stiffness measurements were conducted on the three-axial magnetic levitation force measurement system, including three-axial load cell and laser position sensors with force sensitivity in z- and x-axis of 1 and 0.5 N, respectively, and position sensitivity interval in z- and x-axes of 0.013–0.125 mm.[37]

The magnetic levitation force (F_z) and vertical stiffness (k_z) measurements were conducted in different field cooling heights (FCHs) of 5, 25, and 55 mm, while the lateral guidance force measurements were conducted in FCHs of 5 and 10 mm at a constant working height (WH) of 10 mm. For the vertical levitation force measurements, the YBCOs, with a critical temperature of about 92 K, are cooled by filling the HTS vessel with liquid nitrogen (77 K) and adding liquid nitrogen into the vessel for 15 min to reach thermal stabilisation. After the cooling process, the vertical levitation force data is collected while the vertical distance between the PMG and HTS units increases from the related FCH to the maximum gap of 55 mm, then to the minimum gap of 5 mm, and finally to 55 mm again. For the guidance force (F_x) measurements, the YBCOs are cooled in related FCH. Then the vertical gap between the HTS and PMG units is set to the WH of 10 mm and the lateral force data is collected while the lateral distance (x) changes from the initial central position (0) to +10 mm, then −10 mm and finally to +10 mm depending on the coordinate system shown in Figure 1.

3 | RESULTS AND DISCUSSION

The numerically obtained magnetic flux density distributions by COMSOL Multiphysics from 5 mm above the upper surface of three different PMGs are given in Figure 2. One can see that PMG-A has the biggest B_x and B_z values while PMG-B has the smallest ones. The highest magnetic flux distribution of PMG-A is a result of the special arrangement of this PMG to concentrate most of the magnetic flux on its desired surface, similar to the generally used Halbach PMG[33] with five PMs. As seen in Figure 1, the only difference between PMG-B and PMG-C is a 5 mm gap between the PMs. This difference caused an increment in B_z of PMG-C, as seen in Figure 2. Almost at all of the x distance range, the slope and thus the gradient of the magnetic flux density curves of PMG-B and PMG-C are nearly the same. However, the 5 mm gap between the PMs in PMG-C enables us to put the sliced HTS pieces on the peak positions of the corresponding PMs below. This situation is expected to be beneficial for obtaining higher levitation and guidance forces, as discussed below.

Since the bulk samples may have different porosity densities depending on the depth from the surface, affecting the structural and the superconducting properties of the YBCO, investigating the hole densities on the sliced pieces is important. The optical photograph and the porosity analysis of the middle and bottom slices of the YBCO are shown

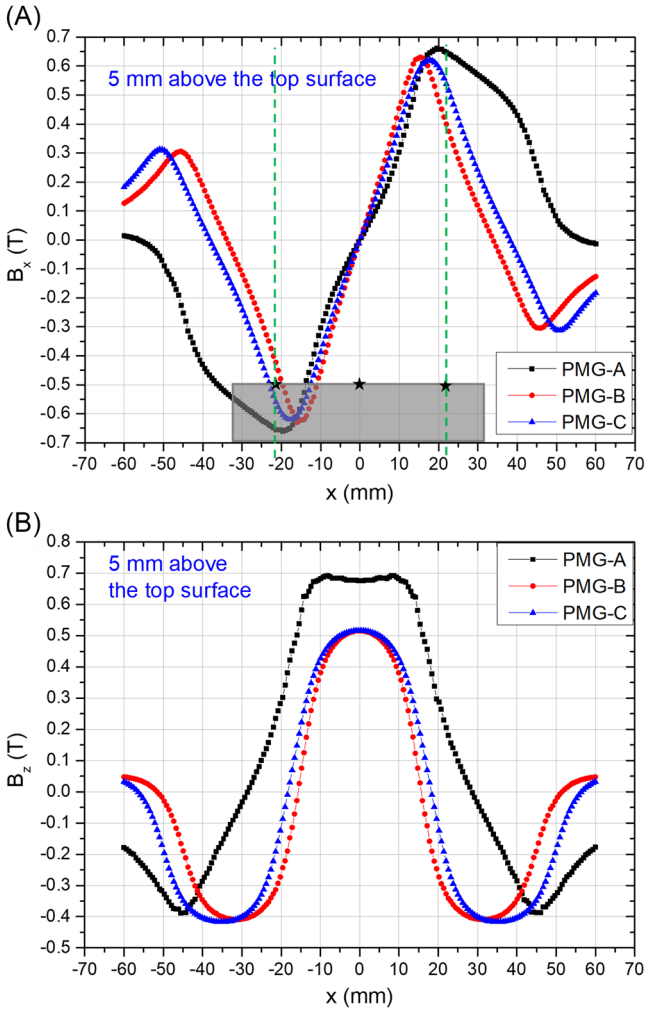

FIGURE 2 B_x (A) and B_z (B) magnetic flux density distributions of the permanent magnetic guideways (PMGs). The dotted green lines show the seed positions on the YBCO.

in Figure 3. The left image is the optical photograph taken from the sliced surface, and the right image represents the hole map in different colors on the same surface of the sliced YBCO. The red regions represent the holes of a diameter bigger than 0.5 mm, while the blue regions represent the holes of a diameter smaller than 0.5 mm. The top slice of the whole YBCO was not shown here since the upper surface of this slice has a massive structure, and the bottom surface corresponds to the M-sliced piece. The porosity properties of the M-Sliced YBCO and B-Sliced YBCO are shown in Table 1. The ratio of holes that has a smaller diameter than 0.5 mm to the total number of holes is almost unchanged, while the ratio of the hole area to the related sliced surface area decreases significantly as going to the deeper region in the YBCO.

To determine the best PMG arrangement and YBCO lying mode (longitudinally, Ln and transversally, Tr) for higher levitation and guidance forces together, we have constructed three different PMGs, as shown in Figure 1. The levitation force and guidance force comparison of different PMGs by using a whole YBCO are shown in Figure 4. The biggest levitation force was obtained with PMG-A (Tr) arrangement as 171 N, while the biggest guidance force was obtained with PMG-B (Tr) arrangement as −67 N. As seen from the figure, bigger levitation and guidance force are obtained by using the YBCO in transversal lying mode for both PMG-A and PMG-B compared to the longitudinal mode due to more interaction area of the YBCO with the PMG. Although maximum levitation force values obtained with PMG-A and PMG-B in the transversal mode are close, the highest guidance force results are distinctly different in favor of PMG-B. The levitation force in the vertical direction depends on the lateral component of the magnetic flux density according to the equation $F_z = \int J_y B_x \, dV$, where F_z is the levitation force, J_y is the shielding current density on the sample surface, B_x is the lateral component of the magnetic flux density and dV is the volume element. The B_x magnetic flux density of PMG-A and PMG-B are close to each other in the region between the seeds of ± 22 mm, as indicated with dotted green lines in Figure 2A. The higher B_x curve of PMG-A is seen outside the seed region of the YBCO and its effect on the levitation force is relatively small. Therefore, the close levitation force of PMG- A (Tr) and PMG-B (Tr) can be attributed to the close B_x values of these PMGs, as seen in Figure 2A.

The lateral guidance force is related to the trapped magnetic flux in the sample. The pinning force, F_P inside the YBCO is defined as $F_P = J|B|$, where J is the supercurrent density.[38] Since the same YBCO with three seeds is used, the difference in guidance force can result from the external magnetic field sources' properties such as pole direction and number. The bigger B_z peak value of PMG-A at the center of the PMG can trap higher magnetic flux inside the YBCO than PMG-B. However, PMG-B has three magnetic pole peaks at the interaction region of the YBCO-PMG and this three-pole effect induces three supercurrent loops around the seeds inside the YBCO. The flux trapping performance of PMG-B can be defined as the sum of each pole interaction. Although higher pinning force is expected for PMG-A due to higher B_z and thus J, three "$J|B|$" contribution comes from PMG-B configuration because of three supercurrent loops, and therefore, PMG-B shows a bigger guidance force.

To increase the levitation force and energy efficiency of the Maglev systems, total weight should be decreased while the levitation and guidance forces are increased. For this aim, we have sliced the bulk YBCO into three pieces. Figure 5 shows the levitation and guidance force comparison of three different PMGs with the middle slice of the YBCO (M-Slice) in transversal lying mode. The peak points of the levitation force curves are of close value with

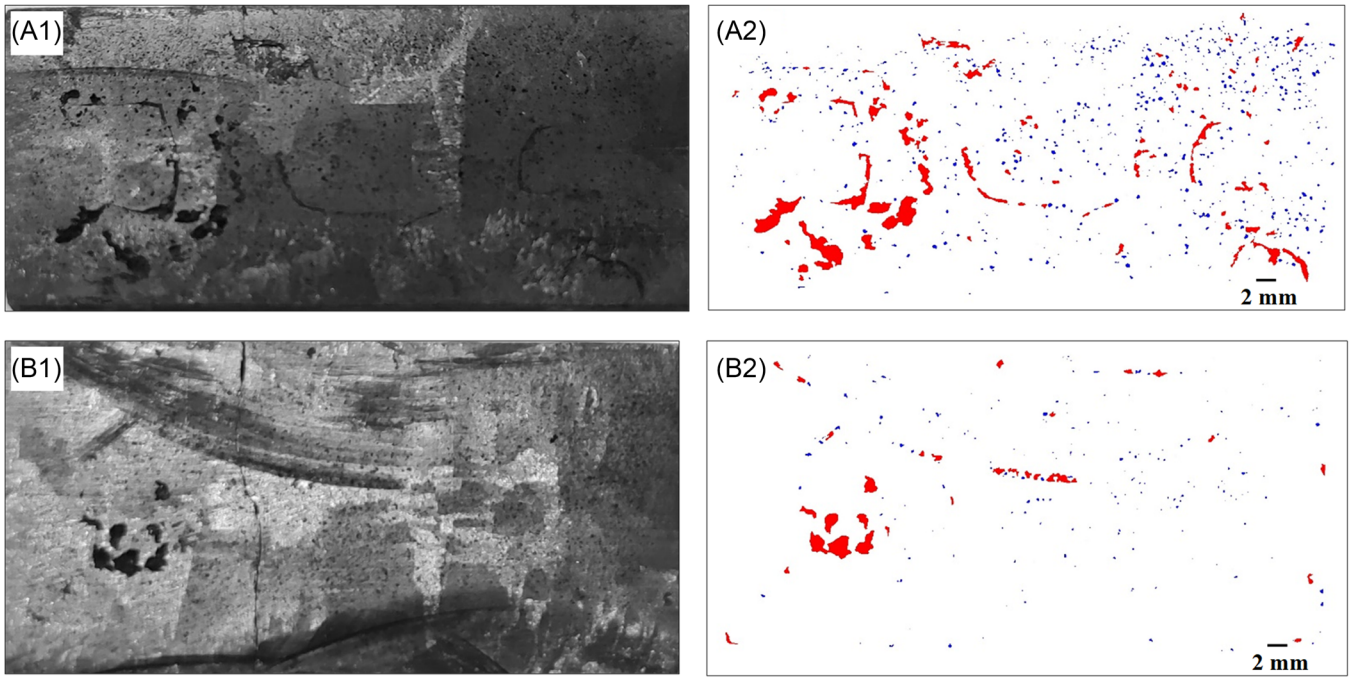

FIGURE 3 The optical photograph and the porosity analysis of the M-Sliced YBCO (A) and B-Sliced YBCO (B).

a noticeable hysteresis difference in the curve of PMG-A. The different behavior of this PMG is manifested as the smallest hysteresis in the guide force curve as opposed to the levitation force, as shown in Figure 5B. It is clearly seen by comparing Figure 4 and Figure 5 that the hysteresis curves of sliced YBCO are distinctly bigger than that of the whole bulk YBCO. This is attributed to the smaller thickness of the sliced YBCO, causing an insufficiency of the shielding currents in the sample and allowing more magnetic flux to enter the sample. Besides, the wider hysteresis curves of PMG-A (Tr) in Figure 5A are a result of the higher B_z value of this PMG, as seen in Figure 2B, causing more magnetic flux entering the sample. The maximum guidance force values of PMG-B (Tr) and PMG-C (Tr) are bigger than that of PMG-A (Tr), as consistent with the explanations on three pole effect related local pinning force of $J|B|$ in Figure 4A.

To get maximum efficiency from a unit YBCO with a mass of 172 g, we have sliced three YBCO samples into three pieces horizontally, as stated in the Experimental section. Levitation and guidance force comparisons of different PMGs by using top (T), middle (M), and bottom (B) slices of the YBCO longitudinally lying above the PMGs in different configurations are shown in Figure 6. A maximum levitation force of 173 N was obtained by PMG-C and a minimum levitation force of 94 N was obtained by PMG-A for the T-T-T configuration, as shown in Figure 6A. It is important to note that the total mass of the three top pieces is 160 g, which is lower than the mass of the whole YBCO due to powder loss during the cutting process. The obtained bigger levitation force of the PMG-C array with the longitudinally lying mode of the T-T-T sliced configuration in Figure 6A is attributed to the structural and electromagnetic harmony of the HTS slices with the PMG pole direction so as to induce higher currents inside the sliced pieces. After determining that the PMG-C arrangement provides the biggest levitation force by using T-T-T sliced HTS, we have investigated the horizontal location effect of the sliced segments taking from the whole YBCO on the levitation and guidance force behavior using M-T-B configuration. In Figure 6B, M-T-B corresponds to three sliced pieces of one whole YBCO with a total mass of 160 g.

TABLE 1 Porosity properties of the M-Sliced YBCO and B-Sliced YBCO.

	M-Slice	B-Slice
Total number of holes on the surface	855	230
Total number of holes that has a smaller diameter than 0.5 mm	776	202
The ratio of the hole area to the sliced surface area (%)	4.53	1.29
The ratio of holes that has a smaller diameter than 0.5 mm to the total number of holes (%)	90.8	87.8

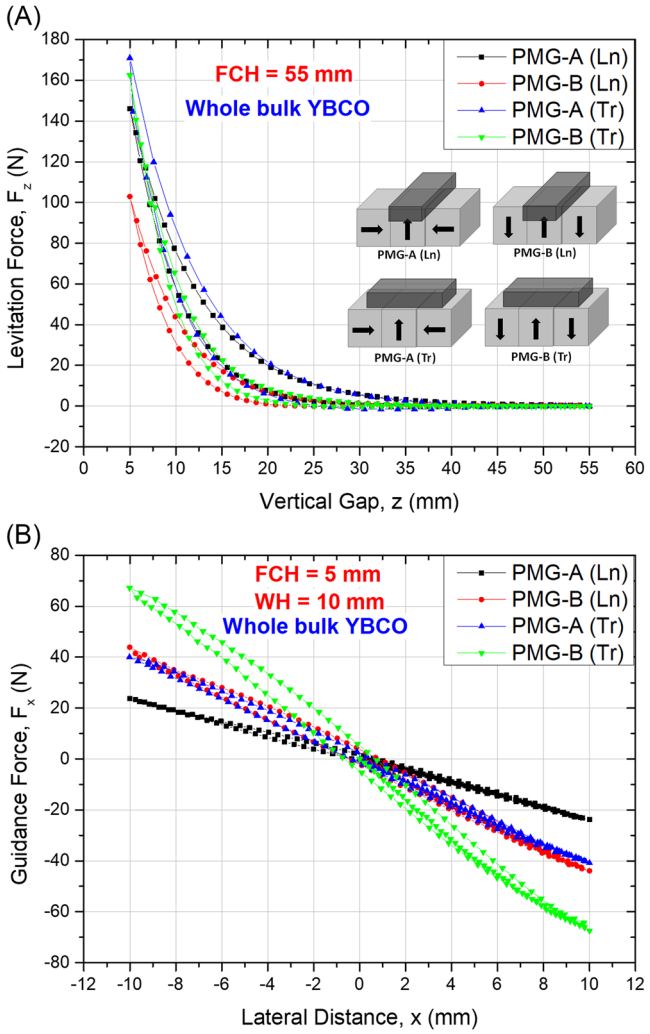

FIGURE 4 Levitation force (A) and guidance force (B) comparison of different PMGs by using a single whole YBCO in traversal and longitudinal lying modes.

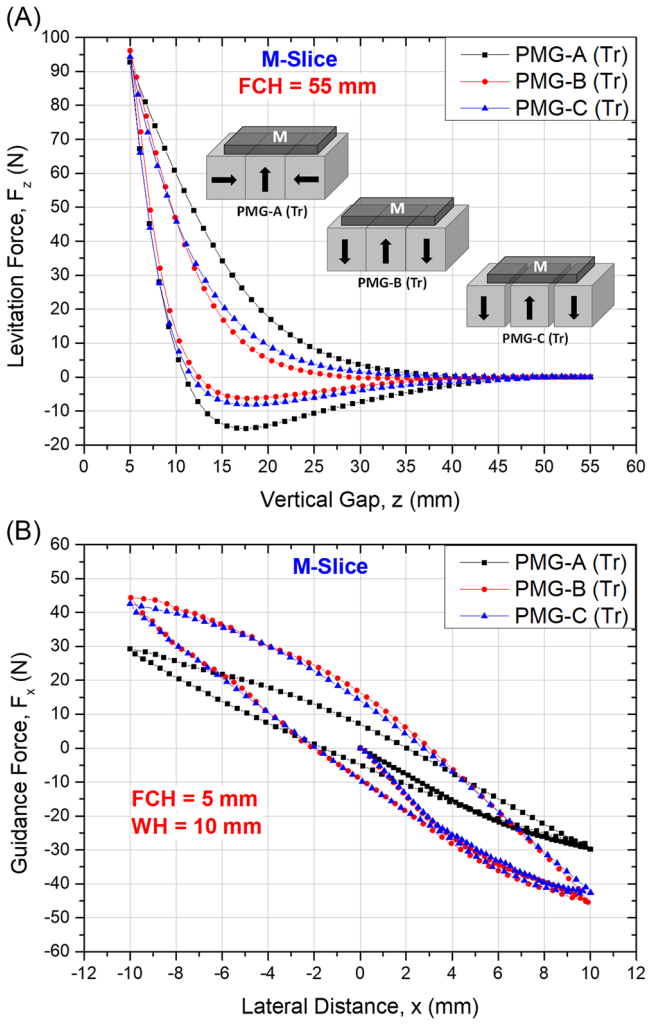

FIGURE 5 Levitation force (A) and guidance force (B) comparison of different PMGs by using the middle slice of the YBCO in transversal lying mode.

By comparing Figure 6A,B, one can see that the maximum levitation force value of the M-T-B configuration of 183 N is slightly bigger than the corresponding value of 173 N with the T-T-T configuration. The slight difference between the levitation forces comes from different micro and electromagnetic properties of the slices at different positions (as M and B) in the whole YBCO as consistent with the literature.[21,39] As seen in Figure 3 and Table 1, the hole number density in the bottom slice is lower than the middle slice of the YBCO. Therefore, the slight increment in the levitation force mentioned above results from the micro-structural enhancement in the bottom slice of the YBCO. Figure 6C shows that the M-T-B configuration's maximum guidance force in FCH = 5 mm is 63 N, while the whole YBCO with PMG-B (Ln) configuration is 44 N. This 43% increment indicates that the guidance force can be improved by utilising the sliced portion. Figure 7 shows the levitation force and guidance force comparison of whole YBCO and set of slices in transversal lying mode. Maximum levitation force in FCH = 55 mm is measured as 171, 162, and 289 N while corresponding guidance force values are measured as 41, 67, and 128 N for PMG-A (Tr)/Whole YBCO, PMG-B (Tr)/Whole YBCO and PMG-B (Tr)/M-T-B configurations, respectively.

Maximum levitation force, guidance, and normalized force values for different configurations in transversal mode are summarized in Table 2. In the table, F_z/m and F_x/m values are calculated by dividing the maximum values of related forces by the total mass of related YBCO. It is seen from the table that the maximum levitation force obtained with sliced YBCO is increased by 69% and 78%, while these increments in guidance force are obtained as 212% and 91%, as compared to the whole YBCO above PMG-A and PMG-B, respectively. On the other hand, the levitation and guidance force density with respect to the total mass of the unit set of slices YBCO increased by 92%

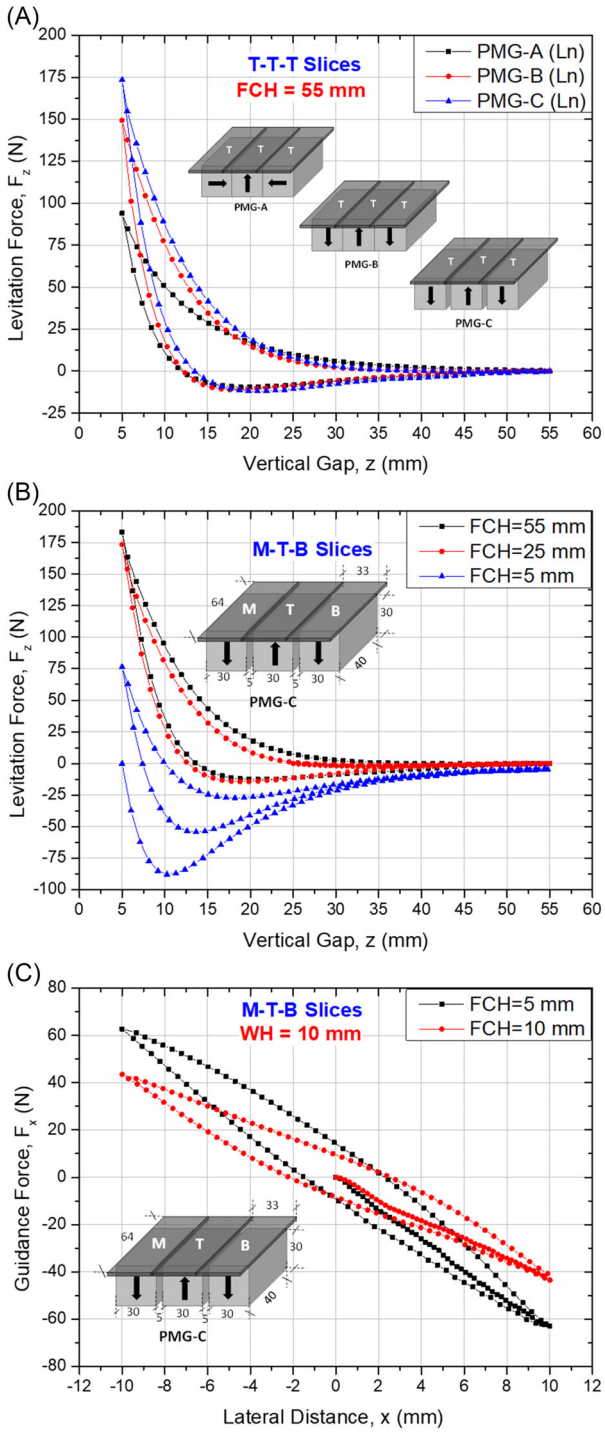

FIGURE 6 Levitation force comparison of permanent magnetic guideway (PMG)-A, PMG-B, and PMG-C by using T-T-T slices in longitudinal lying mode (A), Levitation force (B), and guidance force (C) curves of M-T-B slices in different field cooling heights (FCHs).

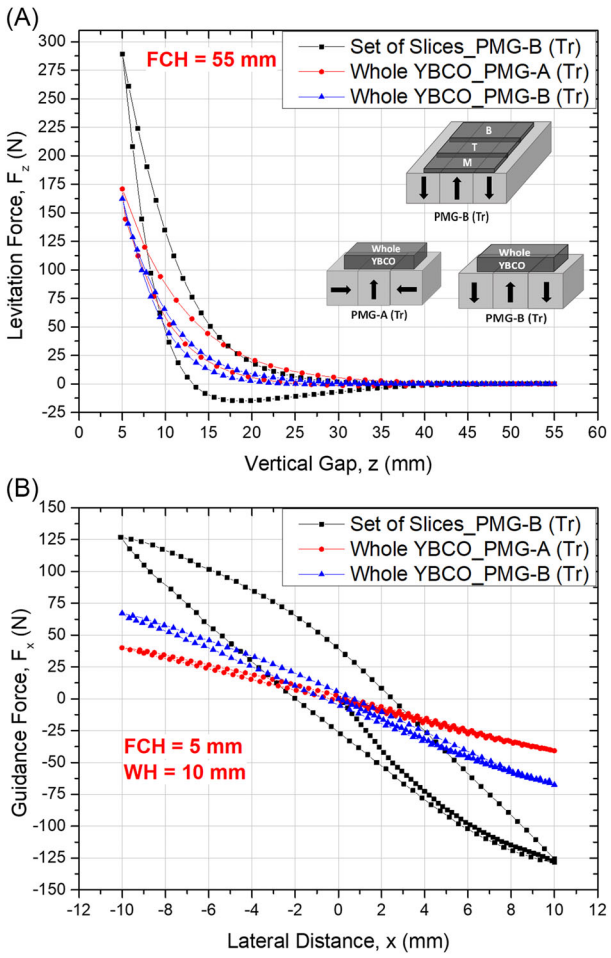

FIGURE 7 Levitation force (A) and guidance force (B) comparison of whole YBCO and set of slices in transversal lying mode.

TABLE 2 Maximum levitation force, guidance, and normalized force values for different configurations in transversal mode.

	PMG-A (Tr)/Whole YBCO	PMG-B (Tr)/Whole YBCO	PMG-B (Tr)/M-T-B
Maximum F_z (N)	171	162	289
Maximum F_x (N)	41	67	128
Total mass, m (g)	172	172	160
F_z/m (N/g)	0.994	0.942	1.81
F_x/m (N/g)	0.238	0.389	0.800

and 106%, respectively, as compared to the whole YBCO above PMG-B in transversal mode. It should be noted that the result in this study is obtained by using PMs with surface magnetic flux densities of 0.53 T. Further investigations should be performed to investigate the effect of slicing on the force and cost efficiency of Maglev systems with bigger magnetic flux density values.

4 | CONCLUSIONS

In this study, we aimed to utilize the PMG surface as much as possible to enhance the force performance of Maglev systems without increasing the HTS number by dividing

the YBCO bulks into three slices horizontally. Firstly, we conducted a porosity analysis of the sliced YBCO parts, and it was observed that the hole number density in the bottom slice is lower than the middle slice of the YBCO. We used whole YBCO above different PMGs in two lying positions of transversal and longitudinal and determined that the levitation and guidance forces measured by using the YBCO in transversal lying mode for both PMG-A and PMG-B are bigger as compared to the longitudinal mode due to more effective interaction area with the PMG.

The maximum levitation force obtained with sliced YBCO is increased by 69% and 78%, while these increments in guidance force are determined as 212% and 91%, as compared to the whole YBCO above PMG-A and PMG-B, respectively. Besides, the levitation and guidance force density with respect to the total mass of the unit set of slices YBCO increased by 92% and 106%, respectively, as compared to the whole YBCO above PMG-B in transversal mode. It is concluded from this study that the levitation and guidance force performance can be increased without increasing the total mass of the onboard unit, by using the sliced YBCO pieces. Since this situation provides time and cost efficiency, the method with sliced YBCO from a whole bulk can increase the technological applicability potential of the Maglev systems.

ACKNOWLEDGMENTS

This work was supported by the Scientific and Technological Research Council of Türkiye (TUBITAK), with project number 122F432, and the Scientific Research Projects Coordination Unit of Karadeniz Technical University with project No. FBA-2021-9814.

ORCID

Murat Abdioglu https://orcid.org/0000-0002-5497-0817

REFERENCES

1. Bednorz JG, Mueller KA. Possible high Tc superconductivity in the Ba—La—Cu—O system. Z Phys B. 1986;64:189–93.
2. Deng Z, Zhang W, Wang Li, Wang Y, Zhou W, Zhao J, et al. A high-speed running test platform for high-temperature superconducting maglev. IEEE Trans Appl Supercond. 2022;32(4):1–5.
3. Kusada S, Igarashi M, Nemoto K, Okutomi T, Hirano S, Kuwano K, et al. The project overview of the HTS magnet for superconducting maglev. IEEE Trans Appl Supercond. 2007;17(2): 2111–6.
4. Schultz L, deHaas O, Verges P, Beyer C, Rohlig S, Olsen H, et al. Superconductively levitated transport system—the Supratrans project. IEEE Trans Appl Supercond. 2005;15(2):2301–5.
5. Sotelo GG, de Oliveira RAH, Costa FS, Dias DHN, de Andrade R, Stephan RM. A full scale superconducting magnetic levitation (maglev) vehicle operational line. IEEE Trans Appl Supercond. 2015;25(3):1–5.
6. Basaran S, Sivrioglu S. Radial stiffness improvement of a flywheel system using multi-surface superconducting levitation. Supercond Sci Technol. 2017;30(3):35008.
7. Strasik M, Hull JR, Mittleider JA, Gonder JF, Johnson PE, McCrary KE, et al. An overview of Boeing flywheel energy storage systems with high-temperature superconducting bearings. Supercond Sci Technol. 2010;23(3):34021.
8. Werfel FN, Floegel-Delor U, Rothfeld R, Riedel T, Goebel B, Wippich D, et al. Superconductor bearings, flywheels and transportation. Supercond Sci Technol. 2012;25(1):14007.
9. Hull JR, Strasik M. Concepts for using trapped-flux bulk high-temperature superconductor in motors and generators. Supercond Sci Technol. 2010;23(12):124005.
10. Weng F, Zhang M, Lan T, Wang Y, Yuan W. Fully superconducting machine for electric aircraft propulsion: study of AC loss for HTS stator. Supercond Sci Technol. 2020;33(10):104002.
11. Elwakeel A, McNeill N, Pena-Alzola R, Zhang M, Yuan W. Cryogenic DC/DC converter for superconducting magnet application. IEEE Trans Appl Supercond. 2022;32(6):1–5.
12. Durrell JH, Dennis AR, Jaroszynski J, Ainslie MD, Palmer KGB, Shi Y-H, et al. A trapped field of 17.6 T in melt-processed, bulk Gd-Ba-Cu-O reinforced with shrink-fit steel. Supercond Sci Technol. 2014;27(8):82001.
13. Vakaliuk O, Werfel F, Jaroszynski J, Halbedel B. Trapped field potential of commercial Y-Ba-Cu-O bulk superconductors designed for applications. Supercond Sci Technol. 2020;33(9):95005.
14. Abdioglu M, Ozturk K, Ekici M, Savaskan B, Celik S, Cansiz A. Design and experimental studies on superconducting maglev systems with multisurface HTS–PMG arrangements. IEEE Trans Appl Supercond. 2021;31(6):1–7.
15. Ozturk K, Badia-Majos A, Abdioglu M, Dilek DB, Gedikli H. Experimental and numerical investigation of levitation force parameters of novel multisurface Halbach HTS–PMG arrangement for superconducting maglev system. IEEE Trans Appl Supercond. 2021;31(7):1–12.
16. Tang R, Song Y, He J, Liu X, Ren Y, Zhou D, et al. Correlation between density and levitation performance of YBCO bulk superconductor over Halbach NDFEB guideway. IEEE Trans Appl Supercond. 2022;32(4):1–4.
17. Zhou D, Zhu L, Liu J, Cai F, Xu T, Wang L, et al. Vertical magnetic field distribution characteristics of triple-peak Halbach array pmg and its engineering application in HTS maglev train. IEEE Trans Appl Supercond. 2022;32(9):1–8.
18. Ozturk K, Guner SB, Abdioglu M, Demirci M, Celik S, Cansiz A. An analysis on the relation between the seed distance and vertical levitation force for the multi—seeded YBCO using the modified advanced frozen image (MAFI) and experimental methods. J Alloys Compd. 2019;805:1208–16.
19. Schatzle P, Krabbes G, Stover G, Schlafer D. Multi-seeded melt crystallization of YBCO bulk material for cryogenic applications. Supercond Sci Technol. 1999;12(2):69–76.
20. Yoo SI, Takebayashi S, Hayashi N, Nagashima K, Sakai N, Murakami M. Seeded melt growth of large lre-ba-cu-0 bulk superconductors. Adv Supercond X. 1998;10:697–700.
21. Guner SB, Celik S, Tomakin M. The investigation of magnetic levitation performances of single grain YBCO at different temperatures. J Alloys Compd. 2017;705:247–52.

22. Floegel-Delor U, Riedel T, Schirrmeister P, Koenig R, Kantarbar V, Liebmann M, et al. Strictly application-oriented REBCO bulk fabrication. J Phys Conf Ser. 2020;1559(1):12046.
23. Shi Y, Kumar Namburi D, Zhao W, Durrell JH, Dennis AR, Cardwell DA. The use of buffer pellets to pseudo hot seed (RE)–Ba–Cu–O–(Ag) single grain bulk superconductors. Supercond Sci Technol. 2016;29(1):15010.
24. Zhou D, Xu K, Hara S, Li B, Deng Z, Tsuzuki K, et al. MgO buffer-layer-induced texture growth of RE–Ba–Cu–O bulk. Supercond Sci Technol. 2012;25(2):25022.
25. Antončík F, Lojka M, Hlásek T, Plecháček V, Jankovský O. Tuning the top-seeded melt growth of REBCO single-domain superconducting bulks by a pyramid-like buffer stack. Ceram Int. 2022;48(4):5377–85.
26. Deng Z, Wang J, Zheng J, Zhang Y, Wang S. An efficient and economical way to enhance the performance of present HTS Maglev systems by utilizing the anisotropy property of bulk superconductors. Supercond Sci Technol. 2013;26(2):25001.
27. Deng Z, Zhang W, Zheng J, Wang B, Ren Y, Zheng X, et al. A high-temperature superconducting maglev-evacuated tube transport (HTS Maglev-ETT) test system. IEEE Trans Appl Supercond. 2017;27(6):1–8.
28. Deng Z, Izumi M, Miki M, Felder B, Tsuzuki K, Hara S, et al. Trapped flux and levitation properties of multiseeded YBCO bulks for HTS magnetic device applications—Part I: Grain and current features. IEEE Trans Appl Supercond. 2012;22(2):6800110.
29. Deng Z, Izumi M, Miki M, Tsuzuki K, Felder B, Liu W, et al. Trapped flux and levitation properties of multiseeded YBCO bulks for HTS magnetic device applications—Part II: Practical and achievable performance. IEEE Trans Appl Supercond. 2012;22(2):6800210.
30. Ozturk K, Kabaer M, Abdioglu M. Effect of onboard PM position on the magnetic force and stiffness performance of multi-seeded YBCO. J Alloys Compd. 2015;644:267–73.
31. Deng Z, He D, Zheng J. Levitation performance of rectangular bulk superconductor arrays above applied permanent-magnet guideways. IEEE Trans Appl Supercond. 2015;25(1):1–6.
32. Ozturk K, Kabaer M, Abdioglu M, Patel A, Cansiz A. Clarification of magnetic levitation force and stability property of multi-seeded YBCO in point of supercurrent coupling effect. J Alloys Compd. 2016;689:1076–82.
33. Halbach K. Application of permanent magnets in accelerators and electron storage rings (invited). J Appl Phys. 1985;57(8):3605–8.
34. Bernstein P, Xing Y, Noudem JG. Increased levitation force in a stable hybrid superconducting magnetic levitation set-up. Eng Res Express. 2022;4(4):45008.
35. Chen N, Chen Y, Sun R, Zheng J, Zheng X, Deng Z. Theoretical model and experiment of the hybrid Maglev vehicle employing high temperature superconducting magnetic levitation and permanent magnetic levitation. Chin Sci Bull. 2020;65(9):847–55.
36. Ozturk UK, Abdioglu M, Mollahasanoglu H. Magnetic force performance of hybrid multisurface HTS maglev system with auxiliary onboard PMs. IEEE Trans Appl Supercond. 2023;33(3):1–6.
37. Ozturk K, Abdioglu M, Karaahmet Z. Magnetic force and stiffness performances of Maglev system based on multi–surface arrangements with three-seeded bulk YBaCuO superconductors. Physica C. 2020;578:1353739.
38. Itoh Y, Mizutani U. Puls Field Magnetization of Melt-Processed Y-Ba-Cu-O Superconducting Bulk Magnet. Jpn J Appl Phys. 1996;35:2114–25.
39. Cardwell DA, Shi Y, Numburi DK. Reliable single grain growth of (RE)BCO bulk superconductors with enhanced superconducting properties. Supercond Sci Technol. 2020;33(2):24004.

How to cite this article: Abdioglu M, Ozturk UK, Guner SB, Ozturk M, Mollahasanoglu H, Yanmaz E. Enhancing magnetic levitation and guidance force and weight efficiency of high-temperature superconducting maglev systems by using sliced bulk YBCO. Int J Appl Ceram Technol. 2023;1–9. https://doi.org/10.1111/ijac.14463